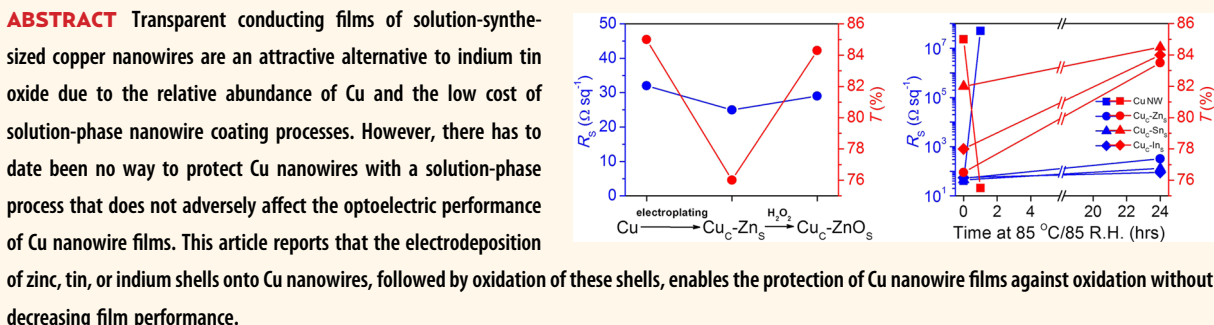


Copper Nanowire Networks with Transparent Oxide Shells That Prevent Oxidation without Reducing Transmittance

Zuofeng Chen,^{†,‡} Shengrong Ye,[‡] Ian E. Stewart,[‡] and Benjamin J. Wiley^{*,‡}

[†]Department of Chemistry, Tongji University, Shanghai 200092, China, and [‡]Department of Chemistry, Duke University, Durham, North Carolina 27708, United States



KEYWORDS: copper nanowires • transparent conductor • core–shell structure • oxidation-resistant • metal oxide

Transparent conducting films are a key component in many applications, including touch screens, e-readers, smart phones, organic solar cells, flat panel displays, and organic light-emitting diodes.¹ Indium tin oxide (ITO) is currently the most widely used transparent conducting film because of its high performance (transmittance on glass >90% at 10 $\Omega \text{ sq}^{-1}$). However, ITO film is mechanically fragile and expensive.^{1,2} The cost arises from both the low abundance of indium in the earth's crust and the slow and inefficient vapor-phase sputtering process required to make high-quality ITO film.² During sputtering, less than 30% of the ITO sputtered from a target ends up on the substrate, which necessitates a recycling infrastructure that adds cost without adding value.³

Films made from one-dimensional (1D) copper nanowires (Cu NWs)^{4–10} are an attractive flexible alternative to ITO because they can be deposited from solution at linear coating rates several orders of magnitude faster than ITO sputtering, offer nearly the same level of optoelectric performance, and are composed of a material that is 1000 times more abundant and 100 times

cheaper than indium ($\$9 \text{ kg}^{-1}$ vs $\$800 \text{ kg}^{-1}$).¹¹ Although solution-coated films of Ag NWs also have an optoelectric performance equivalent to ITO,^{12–17} the price of silver ($\$1000 \text{ kg}^{-1}$) is even greater than that of indium.¹⁸ Given their significant cost advantages, films of Cu NWs are regarded as a promising next-generation transparent conductor. However, Cu NWs are more sensitive to oxidation than Ag NWs, and this fact has hindered their use in applications.

There have been a limited number of studies that aim to address the critical hurdle of protecting Cu NWs from oxidation. One earlier attempt to protect Cu NWs consisted of coating a layer of Ni onto Cu NWs dispersed in ethylene glycol at 120 °C with electroless plating.¹⁹ Films of cupronickel nanowires were 1000 times more resistant to oxidation than films of Cu NWs, but their transmittance was up to 10% lower than films of Cu NWs at a sheet resistance of 60 $\Omega \text{ sq}^{-1}$.¹⁹ This decrease in transmittance was principally due to the fact that the nickel coating increased the diameter of the nanowires, which in turn increased the amount of light blocked by the nanowires at a given area coverage.^{20–23} In a separate

* Address correspondence to benjamin.wiley@duke.edu.

Received for review August 1, 2014 and accepted September 2, 2014.

Published online September 02, 2014
10.1021/nn504308n

© 2014 American Chemical Society

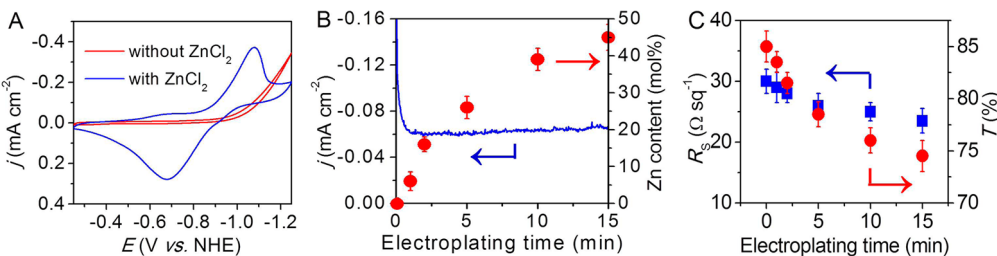


Figure 1. (A) CVs of a Cu NW network in 0.1 M deaerated sodium acetate (pH ~ 8.2) with and without 1 mM ZnCl_2 added to the solution. Scan rate, 100 mV/s. (B) Current and Zn content of the film as a function of electroplating time at -1.15 V vs NHE with 1 mM ZnCl_2 . (C) Plots of sheet resistance and transmittance at $\lambda = 550 \text{ nm}$ vs electroplating time at -1.15 V .

recent report, a layer of aluminum-doped ZnO and Al_2O_3 was deposited on electrospun copper nanofibers by atomic layer deposition (ALD).²⁴ This coating was able to prevent oxidation of the copper nanofibers while decreasing the transmittance of the film at a given sheet resistance by $\sim 1\%$. The main drawback of this approach is that ALD remains a fairly costly technique that is better suited to small-area, high-value devices than large-area, low-cost roll-to-roll production.²⁵

Here we report a solution-phase process for protecting films of Cu NWs from oxidation without degrading their performance. This general approach consists of electroplating a metal, such as Zn, Sn, or In, onto the surface of Cu NWs after film formation, followed by oxidation of the metal coating to create a transparent zinc, tin, or indium oxide shell. These oxide shells protect Cu NWs from oxidation without degrading the transmittance and conductivity of NW networks.

RESULTS AND DISCUSSION

Cu NWs ($>20 \mu\text{m}$ in length and $\sim 70 \pm 25 \text{ nm}$ in diameter) were synthesized in a manner similar to that reported previously and stored in an aqueous solution containing hydrazine (3 wt %) and polyvinylpyrrolidone (1 wt %).²⁶ A thin, uniform film of the NWs was prepared on glass with a Meyer rod by following the procedure reported previously.²⁶ The Cu NW film (65 mg m^{-2}) exhibited a sheet resistance of $32 \Omega \text{ sq}^{-1}$ at a transmittance of 85% at $\lambda = 550 \text{ nm}$ (all transmittance values refer to specular transmittance). The sheet resistance and transmittance of a NW film can be varied by simply changing the areal density of the NWs.²⁶

The Cu NW network was coated with Zn by electroplating $\text{Zn}(\text{II})$ (1 mM ZnCl_2) in 0.1 M deaerated sodium acetate (pH ~ 8.2) at room temperature. As shown in Figure 1A (red curve), the cyclic voltammetry (CV) profile of the Cu NW network in solution without $\text{Zn}(\text{II})$ is relatively featureless from -0.25 to -1.0 V vs NHE (normal hydrogen electrode). The current onset at -1.0 V is from background water reduction. Upon addition of 1 mM ZnCl_2 (blue curve), a redox couple was observed at $E_{\text{p,c}} = -1.08 \text{ V}$ and $E_{\text{p,a}} = -0.68 \text{ V}$ ($E_{\text{p,c}}$ and $E_{\text{p,a}}$ are the cathodic and anodic peak/plateau

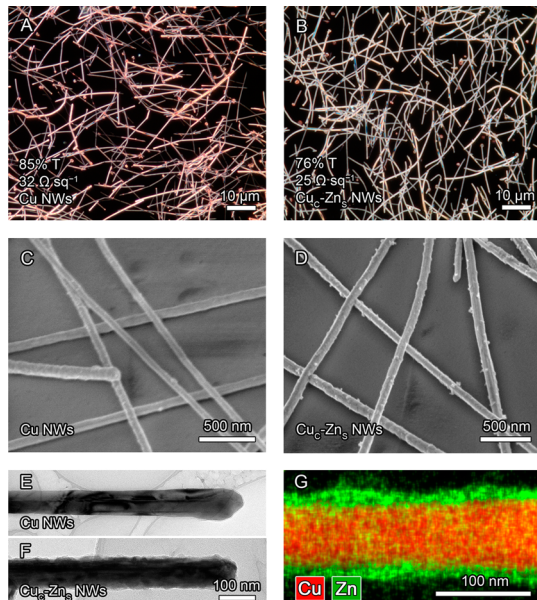


Figure 2. DFOM (A,B), SEM (C,D), and TEM (E,F) images of Cu (A,C,E) and $\text{Cu}_c\text{-Zn}_s$ (39 mol % of Zn) (B,D,F) NWs. (G) EDS mapping image of a $\text{Cu}_c\text{-Zn}_s$ (39 mol % of Zn) NW.

potentials, respectively). The CV behavior is consistent with the electrodeposition of $\text{Zn}(0)$ and the reoxidation of $\text{Zn}(0)$ during the forward and the reverse scans through $\text{Zn}^{2+} + 2e^- \rightleftharpoons \text{Zn}^0$. Continuous electroplating was conducted by holding the potential at -1.15 V , as shown in Figure 1B. Both the transmittance and sheet resistance of the NW networks decreased with increasing Zn content (Figure 1C). For later oxidation studies, we made a Cu–Zn core–shell ($\text{Cu}_c\text{-Zn}_s$) NW network consisting of 39 mol % of Zn (electroplating time = 10 min), which exhibited a sheet resistance of $25 \Omega \text{ sq}^{-1}$ and a transmittance of 76% at $\lambda = 550 \text{ nm}$.

Figure 2 shows dark-field optical microscopy (DFOM), scanning electron microscopy (SEM), transmission electron microscopy (TEM), and X-ray energy-dispersive spectroscopy (EDS) images of the Cu NW and $\text{Cu}_c\text{-Zn}_s$ (39 mol % of Zn) NW networks. The optical images in Figure 2A,B demonstrate that the Cu NWs are evenly dispersed across the glass substrate and interconnected. The color of light scattered from the NWs changes from reddish-orange to neutral gray upon coating with Zn. The electroplating of Zn

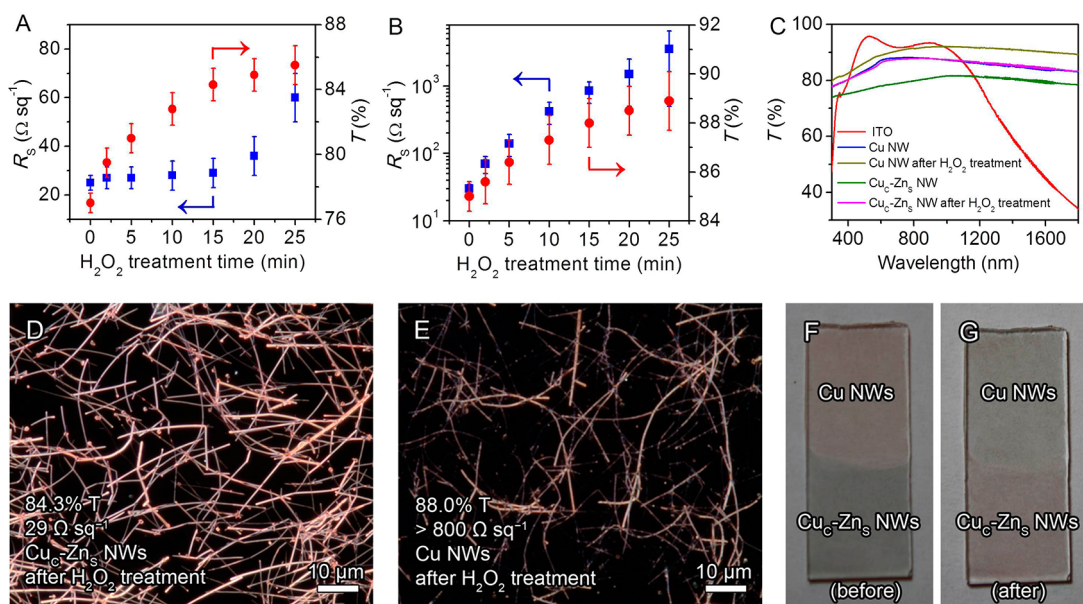


Figure 3. Plots of transmittance ($\lambda = 550$ nm) and sheet resistance of $\text{Cu}_c\text{-Zn}_s$ NWs (A) and Cu NWs (B) vs treatment time in a 2 wt % solution of H_2O_2 in H_2O . (C) Transmittance spectra for ITO ($11 \Omega \text{ sq}^{-1}$), Cu NWs ($32 \Omega \text{ sq}^{-1}$), Cu NWs after H_2O_2 treatment for 15 min ($>800 \Omega \text{ sq}^{-1}$), $\text{Cu}_c\text{-Zn}_s$ NWs ($25 \Omega \text{ sq}^{-1}$), and $\text{Cu}_c\text{-Zn}_s$ NWs after H_2O_2 treatment for 15 min ($29 \Omega \text{ sq}^{-1}$). DFOM images of $\text{Cu}_c\text{-Zn}_s$ (D) and Cu (E) NW films after H_2O_2 treatment for 15 min. Camera photos of $\text{Cu}_c\text{-Zn}_s$ and Cu NW films before (F) and after (G) H_2O_2 treatment for 15 min.

occurred only on the surface of the Cu NWs, with no Zn deposited on the open areas of the substrate. This allowed the network to retain its transmittance after electroplating. The SEM images in Figure 2C,D further confirm that the electroplating occurred only on the surface of the Cu NWs. The surface roughness of the NWs increased after Zn coating, and the average diameter of the NWs increased from ~ 70 to ~ 100 nm. Similar observations were made by TEM images in Figure 2E,F. Cu and Zn have similar atomic masses and therefore do not exhibit much difference in contrast in TEM images. EDS mapping in Figure 2G shows the Cu NW is completely coated with a layer of Zn. The average thickness of the shell was determined to be 15 ± 5 nm after electrodeposition of ~ 39 mol % of Zn.

Unlike Ni coatings,¹⁹ the decrease in the transmittance upon coating of Zn can be recovered. When oxidized, ZnO and/or Zn(OH)₂ is transparent.^{27,28} Figure 3A shows that by dipping the $\text{Cu}_c\text{-Zn}_s$ NW film in H_2O_2 (2 wt %), its transmittance gradually increased to 84.3% after 15 min, a value close to that of the Cu NWs prior to Zn coating (85%), while its sheet resistance remained nearly unchanged. The fact that Zn was electroplated onto the Cu NW network after annealing ensures that the oxidation of the Zn shell does not result in the formation of oxide shells between Cu NWs at their point of electrical contact, and thus there is initially no increase in sheet resistance during the oxidation of Zn. Longer exposures to H_2O_2 resulted in a slight increase in the sheet resistance, potentially due to the oxidation of Cu NWs inside the oxide shell, or alternatively loss of the NWs from the substrate. These results are in contrast to the H_2O_2

treatment of Cu NWs in Figure 3B in which the sheet resistance of the bare Cu NWs increases rapidly after exposure to H_2O_2 , exceeding $800 \Omega \text{ sq}^{-1}$ after 15 min. The full transmittance spectra of films of both bare Cu NWs and $\text{Cu}_c\text{-Zn}_s$ NWs before and after H_2O_2 (2%) treatment for 15 min are shown in Figure 3C.

After H_2O_2 treatment, the DFOM image of NW films in Figure 3D shows that the color of $\text{Cu}_c\text{-Zn}_s$ NWs changes from neutral gray to a Cu NW-like reddish-orange. This is due to the conversion of Zn to a transparent shell consisting of a mixture of ZnO and Zn(OH)₂ (see XPS below). In contrast, the color of Cu NWs in Figure 3E changes from reddish-orange to gray-black due to the oxidation of Cu to CuO, although the oxidized regions of Cu NWs are hardly visible due to the lack of light scattering. The changes in color after H_2O_2 treatment can also be observed in the camera photos in Figure 3F,G.

Unlike films of Cu NWs, the sheet resistance of films of $\text{Cu}_c\text{-Zn}_s$ NWs remains low after extended exposure to conditions designed to accelerate the oxidation of Cu. As shown in Figure 4A, the sheet resistance of Cu NWs increased dramatically in a dry oven at 160°C and becomes insulating ($>10^6 \Omega \text{ sq}^{-1}$) after 12 h. This sheet resistance increase is accompanied by a decrease in the transmittance due to the conversion of Cu NWs to CuO, which has a larger absorption cross section.²⁹ In contrast, the sheet resistance of $\text{Cu}_c\text{-Zn}_s$ NW films increased less than 15% after 18 h, while the transmittance at $\lambda = 550$ nm increased from 76 to 83.6%. Both Cu and $\text{Cu}_c\text{-Zn}_s$ NWs exhibit similar changes in color after heating at 160°C as with the H_2O_2 treatment (Supporting Information Figure S1).

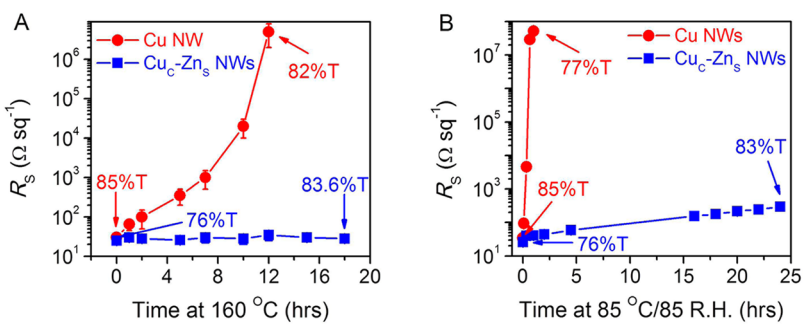


Figure 4. (A) Plots of sheet resistance of Cu_c-Zn_s and Cu NWs vs time in a dry oven at 160 °C. (B) Plots of sheet resistance of Cu_c-Zn_s and Cu NWs vs time at 85 °C/85% RH.

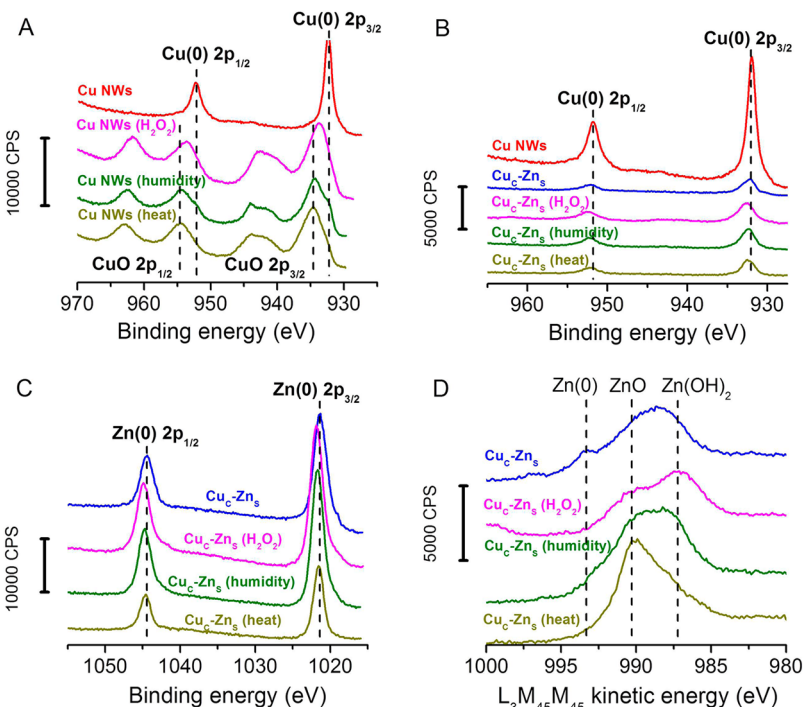


Figure 5. (A) XPS spectra of Cu species present on Cu NWs. (B) XPS spectra of Cu species present on Cu_c-Zn_s NWs. (C) XPS spectra of Zn species present on Cu_c-Zn_s NWs. (D) Auger spectra of Zn species (L₃M₄₅M₄₅ peak) present on Cu_c-Zn_s NWs. The Cu and Cu_c-Zn_s NWs were exposed to a 2 wt % solution of H₂O₂ in H₂O for 15 min, a dry oven at 160 °C for 18 h, or at 85 °C/85% RH for 24 h.

As shown in Figure 4B, similar results were obtained when the films were tested in a humidity chamber at 85 °C with a relative humidity of 85% (85 °C/85% RH). The sheet resistance of Cu NWs increased more rapidly under humid conditions, even given the lower temperature, becoming insulating in less than 30 min. The increase in sheet resistance is much slower for Cu_c-Zn_s NWs; the sheet resistance increased from 25 to \sim 300 $\Omega \text{ sq}^{-1}$ in 24 h. The transmittance of the Cu_c-Zn_s NWs increases by 7% over the test period and is accompanied by a color change from gray to reddish-orange (Supporting Information Figure S2).

We performed X-ray photoelectron spectroscopy (XPS) on both Cu and Cu_c-Zn_s NWs to further characterize their compositional changes after exposure to H₂O₂, elevated temperatures, and humidity. XPS of Cu NWs in Figure 5A exhibits peaks at 932.4 and 952.2 eV,

characteristic of the 2p_{3/2} and 2p_{1/2} binding energies of Cu(0) metal.³⁰ After exposure to H₂O₂, elevated temperatures, or humidity, the 2p peaks shift toward higher binding energy and additional rounded peaks from CuO appeared at 943.6 and 962.4 eV.³⁰

Figure 5B shows that after coating Cu NWs with a layer of Zn, the signals for Cu(0) decrease by approximately 8 times. After H₂O₂ treatment, heat, or humidity tests, these Cu(0) signals are nearly unchanged with no observable development of CuO signals, consistent with the fact that Cu NWs are protected from oxidation by the Zn layer.

Figure 5C shows XPS spectra for the 2p_{3/2} and 2p_{1/2} signals of Zn(0) and Zn(II) from Cu_c-Zn_s NWs before and after exposure to H₂O₂, elevated temperatures, and humidity. There is a small shift of the peaks toward higher binding energies after the various exposures to

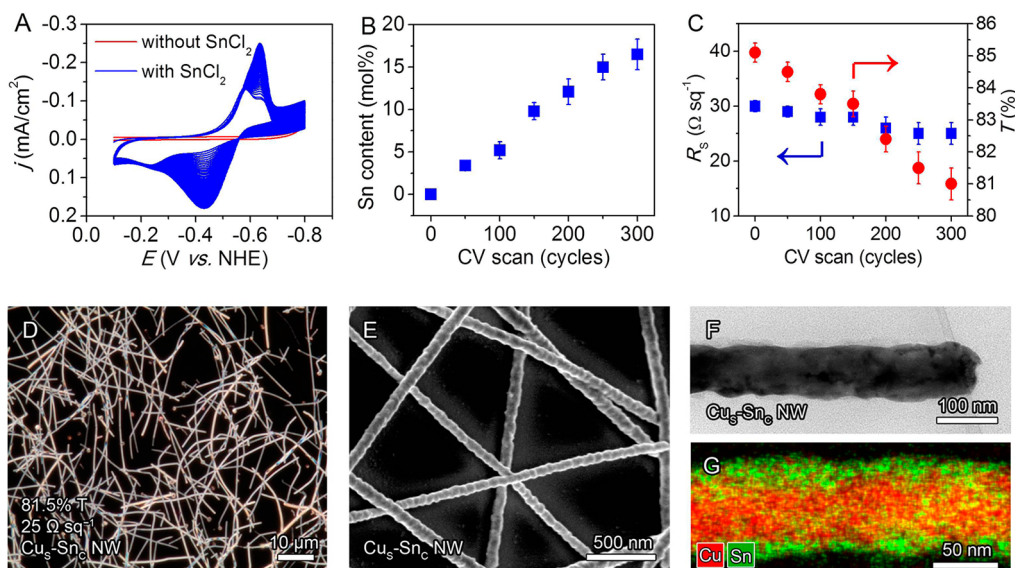


Figure 6. (A) CVs (250 CV scan cycles, scan rate = 100 mV/s) of a Cu NW network in 0.2 M deaerated phosphate buffer (pH 7.0) with and without 1 mM SnCl_2 added to the solution. (B) Sn content of the film as a function of CV scan cycles. (C) Plots of sheet resistance and transmittance at $\lambda = 550$ nm vs scan cycles. (D) DFOM, (E) SEM, (F) TEM, and (G) EDS mapping images of $\text{Cu}_c\text{-Sn}_s$ NWs after 250 CV scan cycles.

oxidizing conditions, qualitatively consistent with the conversion of $\text{Zn}(0)$ to $\text{Zn}(\text{II})$ species given the small spectral difference between $\text{Zn}(0)$ and $\text{Zn}(\text{II})$.^{30,31} In order to see the change in composition more clearly, we show Auger spectra in Figure 5D. $\text{Cu}_c\text{-Zn}_s$ NWs exhibit both a small $\text{Zn}(0)$ peak at 993.4 eV and a broad $\text{Zn}(\text{II})$ peak centered at 988.6 eV, the latter consistent with the surface oxidation of Zn. After exposure to H_2O_2 , heat, or humidity, the peak related to $\text{Zn}(0)$ disappeared but different $\text{Zn}(\text{II})$ species appeared depending on the oxidation conditions. Exposure to H_2O_2 results in two peaks, one due to $\text{Zn}(\text{OH})_2$ and the other due to ZnO .³⁰ After being heated at 160 °C for 18 h, ZnO is the dominant species on the surface of the nanowires. After testing at 85 °C/85% RH for 24 h, both the $\text{Zn}(\text{OH})_2$ and ZnO peaks have similar intensities. The reaction of Zn and ZnO with water to create $\text{Zn}(\text{OH})_2$ under humid conditions may explain the greater susceptibility of the $\text{Cu}_c\text{-Zn}_s$ NW film to oxidize and increase in resistance during exposure to H_2O_2 and 85% RH compared to the dry oven at 160 °C.

Sn can also be electroplated onto the Cu NWs and then oxidized to create a transparent shell that protects the Cu NWs from oxidation. Initial Sn plating attempts were conducted by holding the film at potentials more negative than -0.65 V in a 0.2 M deaerated phosphate buffer (pH 7.0) containing 1 mM SnCl_2 . However, constant-potential electroplating results in a rough coating consisting of nanoparticles with diameters in the tens to hundreds of nanometers (Supporting Information Figure S3, for example). It seems that constant-potential electroplating causes Sn to deposit preferentially at certain surface sites. To overcome this problem, we alternated between reduction and oxidation of Sn on the surface of the Cu NWs with successive

CV scans. Figure 6A shows successive CVs of a Cu NW film ($32 \Omega \text{ sq}^{-1}$, 85% at $\lambda = 550$ nm) under the same solution conditions. The electroplating of $\text{Sn}(\text{II})$ to $\text{Sn}(0)$ on the nanowires is indicated by the increase in the current from the redox process of $\text{Sn}^{\text{II}} + 2e^- \rightleftharpoons \text{Sn}^0$ between -0.20 and -0.70 V. Figure 6B shows the Sn content of the $\text{Cu}_c\text{-Sn}_s$ NWs as a function of scan cycles, and Figure 6C shows that both the transmittance and the sheet resistance of the NW network decreased with increasing Sn content. The Cu -Sn core-shell ($\text{Cu}_c\text{-Sn}_s$) NW network produced by 250 successive CV scans contained 15 mol % of Sn and exhibited a transmittance of 81.5% at $\lambda = 550$ nm and a sheet resistance of $25 \Omega \text{ sq}^{-1}$.

Figure 6D–F shows DFOM, SEM, and TEM images of $\text{Cu}_c\text{-Sn}_s$ NWs. Similar to that of $\text{Cu}_c\text{-Zn}_s$ NWs, the electroplating of Sn occurred only on the surface of the Cu NWs, with no Sn deposited on the open areas of the substrate, and the color of light scattered from the NWs changes from reddish-orange to neutral gray upon coating with Sn. EDS mapping in Figure 6G shows that the Cu NW is largely coated with a thin layer of Sn. The average thickness of the shell was determined to be 3–5 nm after electrodeposition of ~15 mol % of Sn. Comparison of the images in Figure 6 with those in Supporting Information Figure S3 shows that coating Sn with successive reduction and oxidation scans results in a much smoother coating than constant reduction.

Figure 7A shows that coating as little as 5.2 mol % of Sn (100 CV scan cycles) can greatly reduce the oxidation of Cu NWs in a humid environment at 85 °C/85% RH. The resistance to oxidation increases with increasing Sn content up to ~15 mol % of Sn (250 CV scan cycles), at which point the sheet resistance of the $\text{Cu}_c\text{-Sn}_s$ NW film increases by only $105 \Omega \text{ sq}^{-1}$

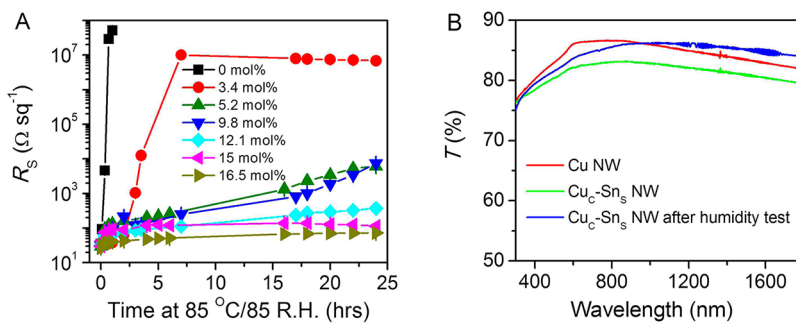


Figure 7. (A) Plots of sheet resistance (R_s) of $\text{Cu}_c\text{-Sn}_s$ NWs of different Sn contents vs time at $85^\circ\text{C}/85\%$ RH. (B) Plots of transmittance vs wavelength for Cu NWs, $\text{Cu}_c\text{-Sn}_s$ NWs (15 mol % of Sn), and $\text{Cu}_c\text{-Sn}_s$ NWs (15 mol % of Sn) after exposure to $85^\circ\text{C}/85\%$ RH for 24 h.

(from 25 to $\sim 130 \Omega \text{ sq}^{-1}$) after 24 h. The XPS spectra in Supporting Information Figure S4A show that Cu(0) $2p_{1/2}$ and $2p_{3/2}$ peaks decrease by approximately 6 times after Sn coating and are retained after the humidity test, whereas Supporting Information Figure S4B shows that the Sn(0) $3d_{3/2}$ and $3d_{5/2}$ peaks completely disappear after the humidity test, consistent with the conversion of Sn(0) to SnO_2 and/or $\text{Sn}(\text{OH})_4$.³⁰ The oxidation of Sn during the humidity test results in an increase in the transmittance of the $\text{Cu}_c\text{-Sn}_s$ NW film from 81.5 to 83.8%. The full transmittance spectra of Cu NWs, $\text{Cu}_c\text{-Sn}_s$ NWs, and $\text{Cu}_c\text{-Sn}_s$ NWs after 24 h at $85^\circ\text{C}/85\%$ RH in Figure 7B show that oxidation of the Sn shell allows the films to recover a significant portion of the transmittance loss after the initial Sn coating.

A similar strategy of electroplating followed by oxidation can also be applied to In to create transparent shells that protect the Cu NWs from oxidation. A Cu NW network ($32 \Omega \text{ sq}^{-1}$, 85% at $\lambda = 550 \text{ nm}$) was coated with In by electroplating In(III) (1 mM InCl_3) onto the Cu NW networks in an aqueous solution of 0.2 M NaCl. The CV in Supporting Information Figure S5A shows a redox couple corresponding to $\text{In}^{\text{III}} + 3e^- \rightleftharpoons \text{In}^0$. Continuous electroplating was conducted by holding the potential at -0.75 V vs NHE for 12 min, resulting in a $\text{Cu}_c\text{-In}_s$ NW network with a transmittance of 78% at $\lambda = 550 \text{ nm}$ and a sheet resistance of $26 \Omega \text{ sq}^{-1}$.

METHODS

All experimental details are included in the Supporting Information.

Conflict of Interest: The authors declare no competing financial interest.

Acknowledgment. This work was supported by funding from Merck KGaA, Darmstadt, Germany. The authors acknowledge the use of the Analytical Instrumentation Facility (AIF) at North Carolina State University, which is supported by the State of North Carolina and the National Science Foundation.

Supporting Information Available: Experimental details for the material preparation, characterization, and testing along with additional supporting data. This material is available free of charge via the Internet at <http://pubs.acs.org>.

The corresponding DFOM and SEM images are shown in Supporting Information Figure S5B,C. Plots of the sheet resistance of the films versus time at $85^\circ\text{C}/85\%$ RH show that this $\text{Cu}_c\text{-In}_s$ NW film is also highly resistant to oxidation (Supporting Information Figure S6); the sheet resistance of the film increased by only $64 \Omega \text{ sq}^{-1}$ (from 26 to $\sim 90 \Omega \text{ sq}^{-1}$) in 24 h. Meanwhile, the transmittance increased from 78 to 83% due to the conversion of In to a transparent layer of In oxide (Supporting Information Figure S7).

CONCLUSIONS

In summary, this study reports a general strategy for protecting copper nanowire films against oxidation with a solution-phase process, without decreasing the optoelectric performance of the film. Coating Cu NWs with a complete shell of Zn, Sn, or In leads to a decrease in the transmittance of the film by 4–9%, but this transmittance loss can largely be recovered by exposing the core–shell nanowires to oxidizing conditions. For example, exposure of a $\text{Cu}_c\text{-Zn}_s$ NW film to H_2O_2 (2 wt %) for 15 min increases the transmittance of the film from 76 to 84% and the sheet resistance from 24 to $29 \Omega \text{ sq}^{-1}$. This work addresses a major practical hurdle to the practical utilization of Cu NW films in touch screens, organic light-emitting diodes, thin-film solar cells, and other optoelectric devices.

REFERENCES AND NOTES

- Gordon, R. G. Criteria for Choosing Transparent Conductors. *MRS Bull.* **2000**, 25, 52–57.
- U.S. Geological Survey *Mineral Commodity Summaries. Indium* **2011**, 74.
- <http://www.nanomarkets.net>; Indium Tin Oxide and Alternative Transparent Conductor Markets.
- Lieber, C. M.; Wang, Z. L. Functional Nanowires. *MRS Bull.* **2007**, 32, 99–108.
- Xia, Y.; Yang, P.; Sun, Y.; Wu, Y.; Mayers, B.; Gates, B.; Yin, Y.; Kim, F.; Yan, H. One-Dimensional Nanostructures: Synthesis, Characterization, and Applications. *Adv. Mater.* **2003**, 15, 353–389.
- Fan, Z.; Ho, J. C.; Takahashi, T.; Yerushalmi, R.; Takei, K.; Ford, A. C.; Chueh, Y.-L.; Javey, A. Toward the Development of Printable Nanowire Electronics and Sensors. *Adv. Mater.* **2009**, 21, 3730–3743.

7. Jin, M.; He, G.; Zhang, H.; Zeng, J.; Xie, Z.; Xia, Y. Shape-Controlled Synthesis of Copper Nanocrystals in an Aqueous Solution with Glucose as a Reducing Agent and Hexadecylamine as a Capping Agent. *Angew. Chem., Int. Ed.* **2011**, *50*, 10560–10564.
8. Chang, Y.; Lye, M. L.; Zeng, H. C. Large-Scale Synthesis of High-Quality Ultralong Copper Nanowires. *Langmuir* **2005**, *21*, 3746–3748.
9. Guo, H. Z.; Lin, N.; Chen, Y. Z.; Wang, Z. W.; Xie, Q. S.; Zheng, T. C.; Gao, N.; Li, S. P.; Kang, J. Y.; Cai, D. J.; et al. Copper Nanowires as Fully Transparent Conductive Electrodes. *Sci. Rep.* **2013**, *3*, 2323.
10. Ye, S.; Rathmell, A. R.; Stewart, I. E.; Ha, Y.-C.; Wilson, A. R.; Chen, Z.; Wiley, B. J. A Rapid Synthesis of High Aspect Ratio Copper Nanowires for High-Performance Transparent Conducting Films. *Chem. Commun.* **2014**, *52*, 2562–2564.
11. U.S. Geological Survey *Mineral Commodity Summaries. Copper* **2011**, 48.
12. Azulai, D.; Belenkova, T.; Gilon, H.; Barkay, Z.; Markovich, G. Transparent Metal Nanowire Thin Films Prepared in Mesopatterned Templates. *Nano Lett.* **2009**, *9*, 4246–4249.
13. Leem, D.-S.; Edwards, A.; Faist, M.; Nelson, J.; Bradley, D. D. C.; de Mello, J. C. Efficient Organic Solar Cells with Solution-Processed Silver Nanowire Electrodes. *Adv. Mater.* **2011**, *23*, 4371–4375.
14. Lee, J.-Y.; Connor, S. T.; Cui, Y.; Peumans, P. Solution-Processed Metal Nanowire Mesh Transparent Electrodes. *Nano Lett.* **2008**, *8*, 689–692.
15. De, S.; Higgins, T. M.; Lyons, P. E.; Doherty, E. M.; Nirmalraj, P. N.; Blau, W. J.; Boland, J. J.; Coleman, J. N. Silver Nanowire Networks as Flexible, Transparent, Conducting Films: Extremely High DC to Optical Conductivity Ratios. *ACS Nano* **2009**, *3*, 1767–1774.
16. Zeng, X.-Y.; Zhang, Q.-K.; Yu, R.-M.; Lu, C.-Z. A New Transparent Conductor: Silver Nanowire Film Buried at the Surface of a Transparent Polymer. *Adv. Mater.* **2010**, *22*, 4484–4488.
17. Chung, C.-H.; Song, T.-B.; Bob, B.; Zhu, R.; Yang, Y. Solution-Processed Flexible Transparent Conductors Composed of Silver Nanowire Networks Embedded in Indium Tin Oxide Nanoparticle Matrices. *Nano Res.* **2012**, *5*, 805–814.
18. U.S. Geological Survey *Mineral Commodity Summaries. Indium* **2011**, 146.
19. Rathmell, A. R.; Nguyen, M.; Chi, M. F.; Wiley, B. J. Synthesis of Oxidation-Resistant Cupronickel Nanowires for Transparent Conducting Nanowire Networks. *Nano Lett.* **2012**, *12*, 3193–3199.
20. Bergin, S. M.; Chen, Y. H.; Rathmell, A. R.; Charbonneau, P.; Li, Z. Y.; Wiley, B. J. The Effect of Nanowire Length and Diameter on the Properties of Transparent, Conducting Nanowire Films. *Nanoscale* **2012**, *4*, 1996–2004.
21. Khanarian, G.; Joo, J.; Liu, X. Q.; Eastman, P.; Werner, D.; O'Connell, K.; Trefonas, P. The Optical and Electrical Properties of Silver Nanowire Mesh Films. *J. Appl. Phys.* **2013**, *114*, 024302–024314.
22. Sorel, S.; Lyons, P. E.; De, S.; Dickerson, J. C.; Coleman, J. N. The Dependence of the Optoelectrical Properties of Silver Nanowire Networks on Nanowire Length and Diameter. *Nanotechnology* **2012**, *23*, 185201–185209.
23. Nirmalraj, P. N.; Bellew, A. T.; Bell, A. P.; Fairfield, J. A.; McCarthy, E. K.; O'Kelly, C.; Pereira, L. F. C.; Sorel, S.; Morosan, D.; Coleman, J. N.; et al. Manipulating Connectivity and Electrical Conductivity in Metallic Nanowire Networks. *Nano Lett.* **2012**, *12*, 5966–5971.
24. Hsu, P. C.; Wu, H.; Carney, T. J.; McDowell, M. T.; Yang, Y.; Garnett, E. C.; Li, M.; Hu, L. B.; Cui, Y. Passivation Coating on Electrospun Copper Nanofibers for Stable Transparent Electrodes. *ACS Nano* **2012**, *6*, 5150–5156.
25. George, S. M. Atomic Layer Deposition: an Overview. *Chem. Rev.* **2010**, *110*, 111–131.
26. Rathmell, A. R.; Wiley, B. J. The Synthesis and Coating of Long, Thin Copper Nanowires To Make Flexible, Transparent Conducting Films on Plastic Substrates. *Adv. Mater.* **2011**, *23*, 4798–4803.
27. Klingshirn, C. ZnO: Material, Physics and Applications. *ChemPhysChem* **2007**, *8*, 782–803.
28. Zarebska, K.; Kwiatkowski, M.; Gniadek, M.; Skompska, M. Electrodeposition of Zn(OH)₂, ZnO Thin Films and Nanosheet-like Zn Seed Layers and Influence of their Morphology on the Growth of ZnO Nanorods. *Electrochim. Acta* **2013**, *98*, 255–262.
29. Wang, Z. M. *Toward Functional Nanomaterials*; Springer: Berlin, 2010; p 51.
30. Wanger, C. D.; Riggs, W. M.; Davis, L. E.; Moulder, J. F.; Muilenberg, G. E. *Handbook of X-ray Photoelectron Spectroscopy: A Reference Book of Standard Data for Use in X-ray Photoelectron Spectroscopy*; Perkin-Elmer Corp.: Eden Prairie, MN, 1979; pp 82, 84, 118.
31. Shang, X. L.; Zhang, B.; Han, E. H.; Ke, W. The Effect of 0.4 wt.% Mn Addition on the Localized Corrosion Behaviour of Zinc in a Long-Term Experiment. *Electrochim. Acta* **2012**, *65*, 294–304.